Table 1. Expression profiles of extracellular matrix–related genes in the presence or absence of IL-20 in the PCR array*

Gene symbol	Gene name	Fold change
Genes up-regulated by IL-20		
THBS2	Thrombospondin 2	113.77
TGIF1	TGFB-induced factor homeobox 1	57.28
MMP9	Matrix metallopeptidase 9	33.13
Genes down-regulated by IL-20		
MMP3	Matrix metallopeptidase 3	0.02
SERPINA1	Serpin peptidase inhibitor, clade A, member 1	0.02
SMAD3	SMAD family member 3	0.02
DCN	Decorin	0.03
PLAU	Plasminogen activator, urokinase	0.03
LOX	Lysyl oxidase	0.03
COL1A2	Collagen, type I, α2	0.03
ENG	Endoglin	0.05
CAV1	Caveolin 1, caveolae protein, 22 kd	0.05
IL5	Interleukin 5	0.06
FASLG	Fas ligand	0.06
IL10	Interleukin 10	0.06
IL1A	Interleukin 1, α	0.06

* A mixture of equal amounts of mRNAs from 3 normal fibroblasts was prepared in the presence or absence of interleukin-20 (IL-20), and the mRNA expression profile was evaluated using a polymerase chain reaction (PCR) array. Fold change was calculated as $1/2^{(\text{raw Ct of each mRNA} - \text{Ct of housekeeping genes})}$. Genes up- or down-regulated >16-fold by IL-20 stimulation are shown.

IL-20–treated fibroblasts in comparison with untreated cells (Table 1). Among them, human α2(I) collagen gene expression was decreased 0.03-fold by IL-20. Consistent with the array result, quantitative real-time PCR using specific primers for α1(I) or α2(I) collagen and an increased number of samples (n = 7) showed that collagen messenger RNA (mRNA) expression was significantly reduced by IL-20 (Figure 1A). Furthermore, immunoblotting revealed that the protein synthesis of type I collagen was also decreased in a dose-dependent manner by treatment with IL-20, and the decrease was statistically significant ($P < 0.05$) (Figure 1B).

To determine whether the down-regulation of collagen by IL-20 takes place at the transcriptional level or translational level, stability of collagen mRNA was examined. Because the steady-state level of mRNA is controlled by the level of gene transcription and/or the stability of mRNA, de novo mRNA synthesis was blocked by the RNA synthesis inhibitor actinomycin D in normal fibroblasts in the presence or absence of IL-20. As shown in Figure 1C, after actinomycin D treatment, there was no significant difference in the decrease rate of α2(I) collagen mRNA between cells with and those without IL-20. Similarly, when de novo protein synthesis and the expression of proteolytic enzymes were blocked with cycloheximide, IL-20 stimulation had little effect on the half-lives of collagen protein (Figure 1D). Taken together, these results indicate that the stability of collagen mRNA and protein was not altered by IL-20, and proteolytic enzymes were less likely to be involved in the effect of IL-20 on collagen expression. Thus, collagen synthesis is thought to be decreased by IL-20 at the transcriptional level.

Next, to identify the element of the human α2(I) collagen promoter that responds to IL-20 stimulation, we compared activities of serial 5′-deletions of the promoter linked to the CAT reporter gene in the presence or absence of IL-20 in normal fibroblasts (Figure 1E). The full-length −3500 to +58 bp construct and the shorter construct with deletion end points at −353 to +58 bp showed a similar fold decrease of promoter activities by IL-20 relative to the values in untreated fibroblasts (~0.3-fold). The −264 to +58 bp construct and shorter constructs did not respond to IL-20 stimulation, indicating that the element of the α2(I) collagen promoter gene that responds to IL-20 is located between −353 and −264 bp.

This region contains the binding sites for Sp1, Ets family transcription factors (e.g., Ets-1 and Fli-1), and CCAAT/enhancer binding protein β (c/EBPβ) (Figure 1E). According to the results of the PCR array, the expression of c/EBPβ and Sp1 was not affected by IL-20 (not shown). Real-time PCR showed that IL-20 induced the expression of Fli-1 but not that of Ets-1 (Figure 2A). In addition, the protein expression of Fli-1 was also increased by IL-20 (Figure 2B). Fli-1 is thought to share binding sites with Ets-1, and it inhibits α2(I) collagen promoter activity by competing with Ets-1 using an overexpression system in vitro (36,37), indicating that the balance of Ets-1 and Fli-1 controls collagen expression (36,38). We found that the ratio of Ets-1:Fli-1 protein expression was significantly decreased by IL-20. Several lines of evidence revealed that posttranslation modification, such as phosphorylation and acetylation, tightly regulates the protein stability and transcriptional activity of Fli-1 (29). Although both phosphorylation and acetylation of Fli-1 were not changed by IL-20 (Figure 2C), the cytokine increased the association of Fli-1 with the collagen promoter in chromatin immunoprecipitates (Figure 2D). These data indicate that IL-20 increased Fli-1 protein through the induction of Fli-1 mRNA levels directly without the alterations of phosphorylation and acetylation.

We also examined the mRNA expression of other human α2(I) collagen promoter–related molecules by real-time PCR. The expression of c-Myb, c-Fos, and

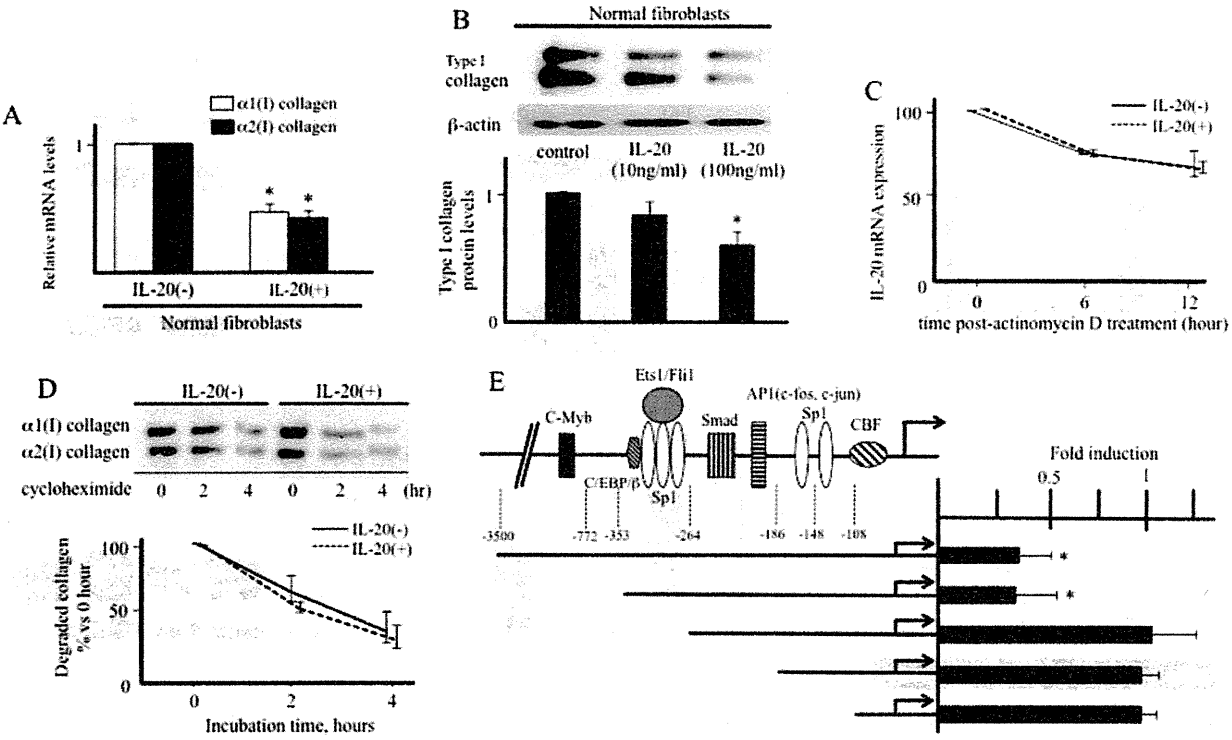

Figure 1. Effect of interleukin-20 (IL-20) on collagen expression. **A,** Normal fibroblasts were treated with IL-20 (100 ng/ml) for 12 hours. Levels of collagen mRNA were determined by real-time polymerase chain reaction (PCR) (n = 7 samples). * = $P < 0.05$ versus untreated fibroblasts (set to 1.0). **B,** Normal fibroblasts were treated with IL-20 (100 ng/ml) for 24 hours. Cell lysates were subjected to immunoblotting. The protein levels of type I collagen quantitated by scanning densitometry and corrected for the levels of β-actin in the same samples are shown relative to those in untreated fibroblasts (set to 1.0) (n = 3 samples). * = $P < 0.05$ versus untreated fibroblasts. **C,** Fibroblasts were incubated in the presence or absence of IL-20 for 12 hours before the addition of 2.5 μg/ml actinomycin D for 6 or 12 hours. IL-20 mRNA expression was analyzed by real-time PCR. **D,** Fibroblasts were incubated in the presence or absence of IL-20 for 24 hours before the addition of cycloheximide (10 μg/ml). Cells were harvested at the indicated time points after cycloheximide was administered, and immunoblotting was performed. The protein levels of type I collagen quantitated by scanning densitometry and corrected for the levels of β-actin in the same samples are shown relative to those in untreated fibroblasts (set to 1.0) (n = 3 samples). **E,** The indicated α2(I) collagen promoter deletion constructs were transfected into normal fibroblasts in the absence or presence of IL-20 (100 ng/ml) for 24 hours (n = 3 samples). The bar graph represents fold stimulation of chloramphenicol acetyltransferase activities stimulated with IL-20 relative to those not stimulated with IL-20 (set to 1.0). * = $P < 0.05$ versus cells not stimulated with IL-20. Values are the mean ± SEM. c/EBPβ = CCAAT/enhancer binding protein β; AP-1 = activator protein 1; CBF = CCAAT-binding transcription factor.

c-Jun was not affected by IL-20 (Figure 2A). Caveolin 1 was down-regulated by IL-20 in the array (Table 1), but the decrease became insignificant in real-time PCR with increasing the number of samples (n = 7) (Figure 2E). Smad3 and endoglin, mediators of TGFβ signaling, were significantly decreased by IL-20 (Figure 2E), consistent with the array results. However, the decrease of Smad3 or endoglin could not explain the reduction of α2(I) collagen expression by IL-20 in normal fibroblasts, because their inhibition was shown to have no effect on basal collagen transcription (39,40). Therefore, our results suggest that IL-20 reduces collagen transcription mainly via Fli-1 expression. Consistent with our hypothesis, the inhibitory effect of IL-20 on collagen was blocked by the transfection of Fli-1 siRNA (Figure 2F).

As described above, IL-19, IL-20, and IL-24 share a receptor (14), although their functions are different. We investigated whether IL-19 and IL-24 also regulate collagen expression in vitro. Immunoblotting revealed that protein synthesis of type I collagen was not significantly affected by treatment with IL-19 or IL-24 in comparison with untreated cells (further information available from the corresponding author). When the ratio of Ets-1:Fli-1 was also examined by immunoblotting, we did not find significant change (further information available from the corresponding author).

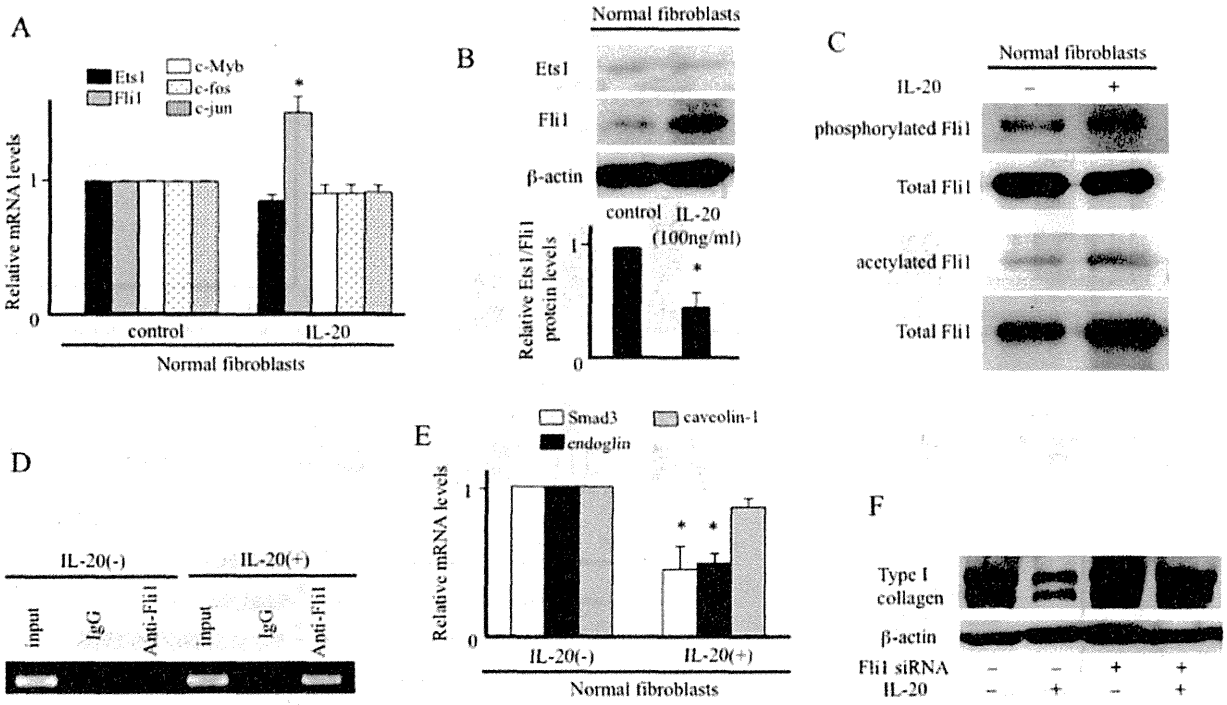

Figure 2. Effect of interleukin-20 (IL-20) on Fli-1 expression. **A,** Normal fibroblasts were incubated in the presence or absence of IL-20 for 12 hours. Messenger RNA levels were determined by real-time polymerase chain reaction (PCR) (n = 7 samples). * = $P < 0.05$ versus untreated fibroblasts (set to 1.0). **B,** Normal fibroblasts were treated with IL-20 for 24 hours. Immunoblotting was performed using antibody to Ets-1 or Fli-1. Protein levels of Ets-1 and Fli-1 were quantitated as described in Figure 1B, and the ratio of Ets-1:Fli-1 protein expression is shown. * = $P < 0.05$ versus untreated fibroblasts (set to 1.0) (n = 3 samples). **C,** Normal fibroblasts were treated with IL-20 (100 ng/ml) for 24 hours. Levels of phosphorylated and acetylated Fli-1 were determined as described in Patients and Methods. **D,** Normal fibroblasts were incubated in the presence or absence of IL-20 for 12 hours. Cellular DNA was sheared, and chromatin (input DNA) was immunoprecipitated with anti–Fli-1 antibody or IgG isotype control antibody. The presence of α2(I) collagen promoter fragments in the precipitates was detected using PCR followed by agarose gel electrophoresis. **E,** Levels of Smad3, endoglin, and caveolin 1 mRNA were determined as described in **A.** * = $P < 0.05$ versus untreated fibroblasts (set to 1.0) (n = 7 samples). **F,** Normal fibroblasts were treated with IL-20 (100 ng/ml) for 12 hours in the presence or absence of Fli-1 small interfering RNA (siRNA). The expression of type I collagen was determined by immunoblotting. Values are the mean ± SEM.

Therefore, among IL-20R–related cytokines, the reduction of collagen expression via Fli-1 up-regulation is likely to be specific to IL-20.

Expression levels of IL-20 in sera and involved skin of patients with SSc. Next, we measured the serum levels of IL-20 in various rheumatic diseases by ELISA. As shown in Figure 3A, the mean serum IL-20 levels in patients with SSc, SLE, and DM were slightly but not significantly decreased compared with those in normal subjects. On the other hand, patients with scleroderma spectrum disorders who did not fulfill the ACR classification criteria for SSc but who we thought would develop SSc in the future (23–25) had IL-20 levels significantly lower than those in normal subjects.

We determined the association of serum IL-20 levels with clinical features and laboratory findings in SSc patients (further information available from the corresponding author). Patients with decreased IL-20 levels (below the average of normal subjects) had a significantly higher prevalence of esophageal involvement than did those with normal IL-20 levels (52.9% versus 12.5%; $P < 0.05$). The modified Rodnan skin thickness score (41) was also increased, although not significantly, in those with decreased IL-20 levels. In contrast, as determined by real-time PCR, IL-20 mRNA expression in involved skin of SSc patients was significantly decreased compared with that in skin of normal subjects (Figure 3B). Immunohistochemical staining using paraffin-embedded skin sections also showed that IL-20 protein was detected strongly in the epidermis of normal skin but hardly detected in SSc atrophic epidermis (Figure 3C). Thus, serum IL-20 levels may be

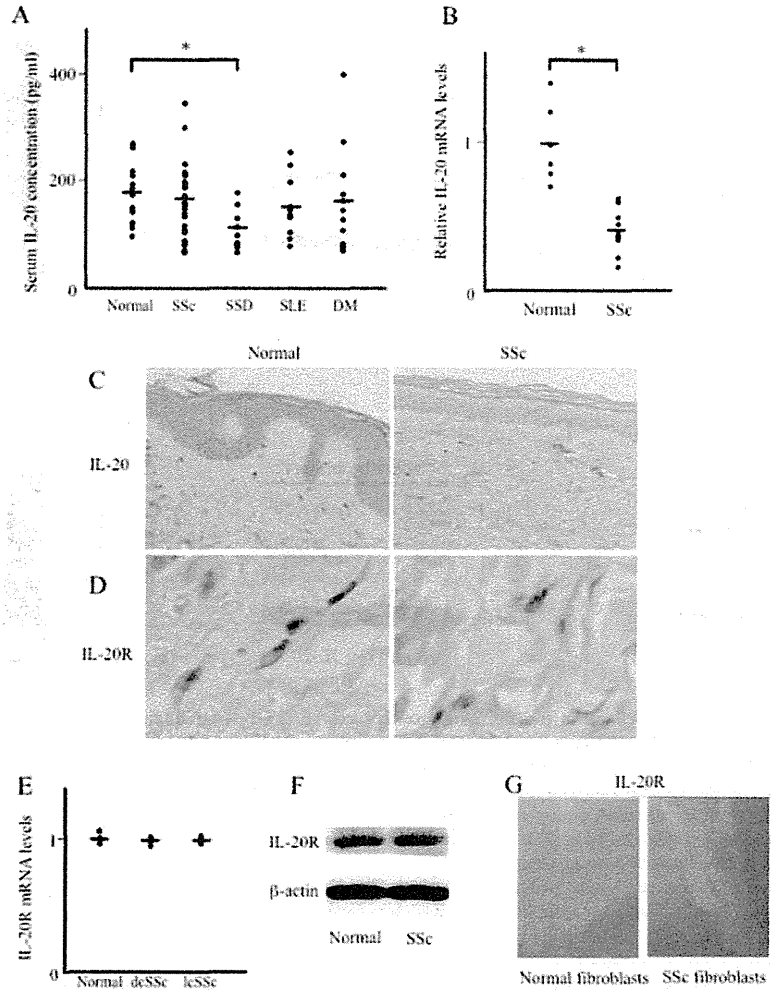

Figure 3. Interleukin-20 (IL-20) levels in sera and skin tissues from patients with rheumatic diseases. **A,** Shown are serum IL-20 levels as determined by enzyme-linked immunosorbent assay. Serum samples were obtained from 33 patients with systemic sclerosis (SSc), 9 patients with scleroderma spectrum disorders (SSD), 10 patients with systemic lupus erythematosus (SLE), 12 patients with dermatomyositis (DM), and 15 normal subjects. Symbols represent individual samples; bars show the mean. * = $P < 0.05$. **B,** Total RNA was extracted from skin tissues obtained from 12 SSc patients and 6 normal subjects. IL-20 mRNA expression was analyzed by real-time polymerase chain reaction (PCR). Symbols represent individual samples; bars show the mean. * = $P < 0.05$. **C,** Paraffin-embedded sections of normal and SSc-involved skin were subjected to immunohistochemical analysis for IL-20. Original magnification × 200 (n = 3 samples). **D,** Paraffin-embedded sections of normal and SSc-involved skin were subjected to immunohistochemical analysis for IL-20 receptor (IL-20R). Original magnification × 400 (n = 3 samples). **E,** Total RNA was extracted, and IL-20R mRNA expression was analyzed by real-time PCR as described in **B.** Symbols represent individual samples; bars show the mean. **F,** Cell lysates were obtained from cultured normal and SSc dermal fibroblasts and subjected to immunoblotting with antibody to IL-20R. Results are representative of 5 normal and 5 SSc fibroblasts. **G,** Expression of IL-20R in cultured normal dermal fibroblasts and SSc fibroblasts was visualized by immunofluorescence microscopy. Original magnification × 1,000. dcSSc = diffuse cutaneous SSc; lcSSc = limited cutaneous SSc.

specifically decreased in the prodromal stage of SSc, while IL-20 expression in involved skin of SSc patients may be constitutively decreased.

Although there has been no previous report indicating that IL-20R is expressed in dermal fibroblasts, immunostaining revealed that IL-20R protein was expressed to a similar extent in fibroblast-like spindle-shaped cells of normal and SSc skin in vivo (Figure 3D). This result was consistent with similar IL-20R expression levels in normal and SSc skin by real-time PCR in vivo

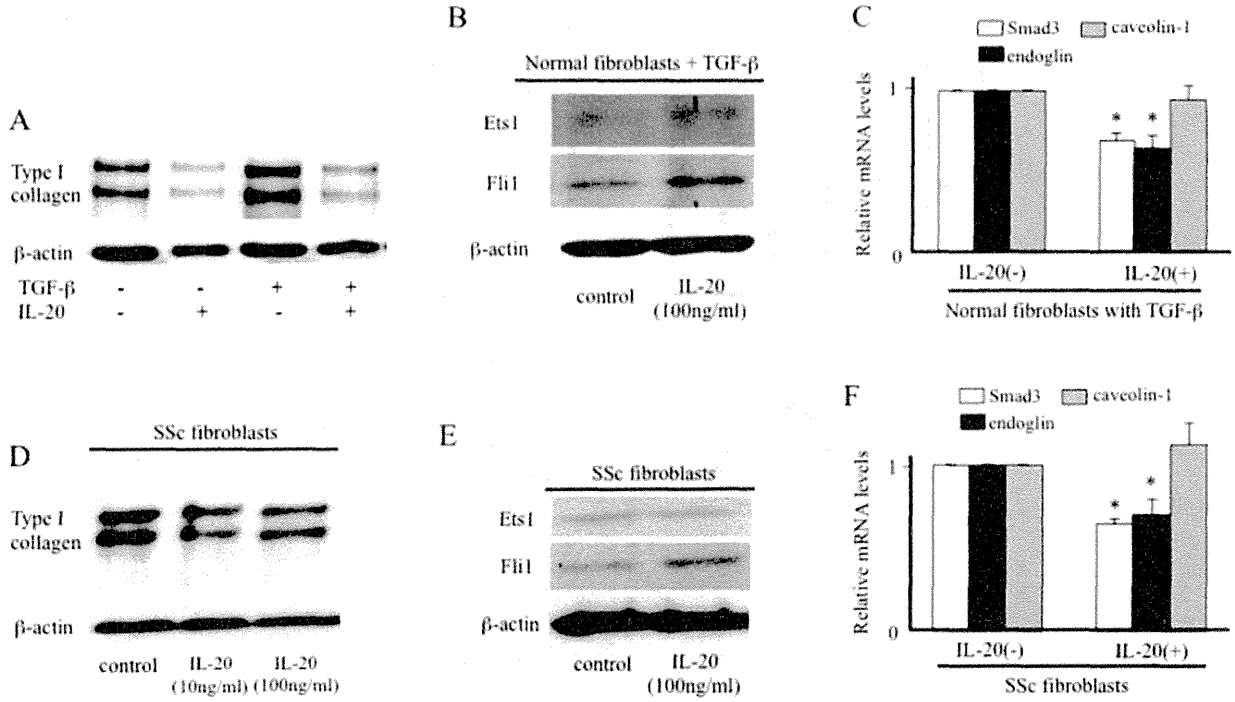

Figure 4. Effect of IL-20 on collagen expression in transforming growth factor β (TGFβ)–stimulated normal fibroblasts or SSc fibroblasts. **A,** Normal fibroblasts were treated with IL-20 (100 ng/ml) and/or TGFβ (2 ng/ml) for 24 hours. The expression of type I collagen was evaluated by immunoblotting. **B,** Normal fibroblasts were treated with IL-20 in the presence of TGFβ (2 ng/ml) for 24 hours. Immunoblotting was performed using antibody to Ets-1 or Fli-1. **C,** Normal fibroblasts were treated with IL-20 (100 ng/ml) for 12 hours in the presence of TGFβ (2 ng/ml). Real-time PCR was performed to evaluate levels of Smad3, endoglin, and caveolin 1 mRNA (n = 7 samples). * = $P < 0.05$ versus untreated fibroblasts (set to 1.0). **D,** SSc fibroblasts were treated with IL-20 for 24 hours. Immunoblotting was performed using antibody to type I collagen. **E,** SSc fibroblasts were treated with IL-20 for 24 hours. Immunoblotting was performed using antibody to Ets-1 or Fli-1. **F,** SSc fibroblasts were treated with IL-20 (100 ng/ml) for 12 hours. Real-time PCR was performed to evaluate levels of Smad3, endoglin, and caveolin 1 mRNA (n = 7 samples). * = $P < 0.05$ versus untreated fibroblasts (set to 1.0). Values are the mean ± SEM. See Figure 3 for other definitions.

(Figure 3E) or by immunoblotting (Figure 3F) and immunofluorescence (Figure 3G) in vitro using cultured fibroblasts. Thus, dermal fibroblasts may express IL-20R, and its expression levels are likely to be similar in normal and SSc fibroblasts. Taken together, these results indicate that IL-20 may have an inhibitory effect on collagen expression, and down-regulation of IL-20 levels in SSc skin in vivo contributes to increased collagen accumulation and tissue fibrosis.

Effect of IL-20 on type I collagen expression in TGFβ-stimulated normal fibroblasts and SSc fibroblasts. We next investigated the effect of IL-20 on type I collagen expression in TGFβ-treated normal fibroblasts. Exogenous IL-20 decreased basal collagen expression, and TGFβ could not induce collagen expression in the presence of IL-20 (Figure 4A), suggesting that IL-20 both suppresses the effect of TGFβ and reduces basal collagen expression. As expected, the protein expression of Fli-1 was increased by IL-20 in the presence of TGFβ (Figure 4B), while the mRNA expression levels of Smad3 and endoglin were decreased significantly (Figure 4C). We assume that IL-20 reduces basal collagen transcription via Fli-1 induction, while the down-regulation of Smad3 and endoglin may cancel the effect of TGFβ. The inhibition of collagen by IL-20 (Figure 4D), the induction of Fli-1 by IL-20 (Figure 4E), and the reduction of Smad3 and endoglin by IL-20 (Figure 4F) were also observed in SSc fibroblasts.

Effect of IL-20 on bleomycin-induced skin fibrosis in mice. Skin fibrosis induced by bleomycin injection in mice is used as a murine model of SSc (33). The epidermis of control mouse skin expressed IL-20, while IL-20 expression was decreased in bleomycin-treated mouse epidermis (Figure 5A), as seen in SSc skin. The expression of IL-20 in inflammatory cells or endothelial cells was slight and similar between control and

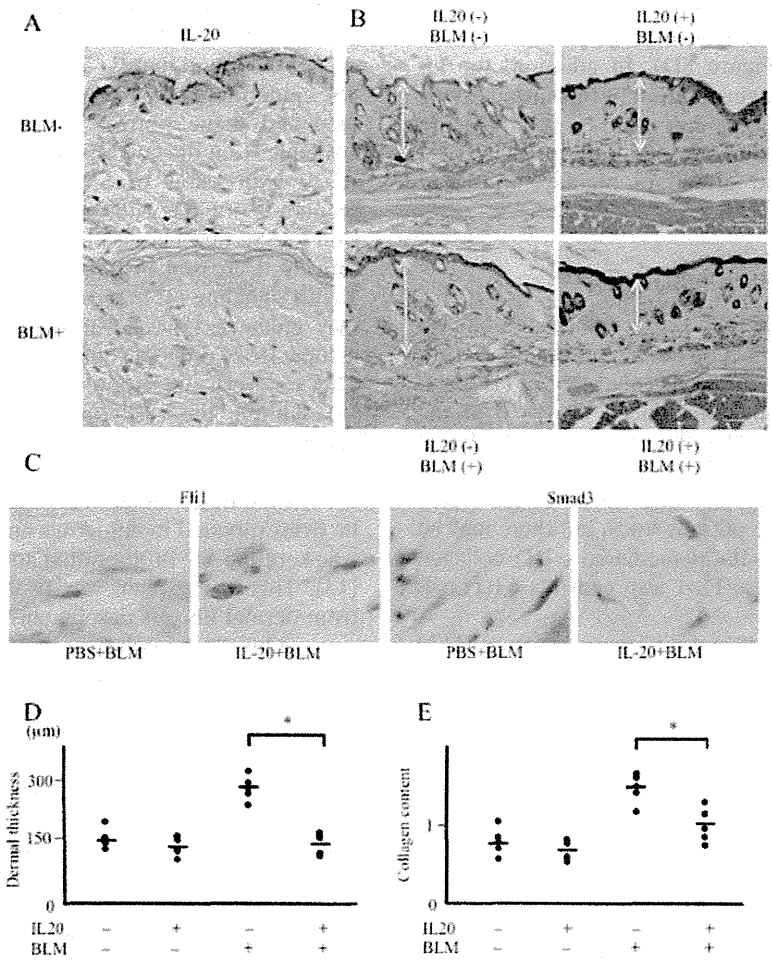

Figure 5. Effect of interleukin-20 (IL-20) on bleomycin (BLM)–induced skin fibrosis in vivo. **A,** Paraffin-embedded sections of skin were subjected to immunohistochemical analysis for IL-20. Top, Phosphate buffered saline (PBS)–treated wild-type mouse. Bottom, Bleomycin-treated mouse. Results shown are representative of 5 samples. Original magnification × 200. **B,** PBS- or bleomycin-treated mouse skin was injected with control PBS (left) or IL-20 (right) and stained with hematoxylin and eosin. **Double-headed arrows** indicate thickness of the dermis. Results shown are representative of 5 samples. Bars = 0.1 mm. **C,** Paraffin-embedded sections of bleomycin-treated mouse skin injected with control PBS or IL-20 were subjected to immunohistochemical analysis for Fli-1 or Smad3. Results shown are representative of 5 samples. Original magnification × 400. **D,** Dermal thickness was measured in PBS- or bleomycin-treated mouse skin injected with control PBS or IL-20 (n = 5 samples per group). Symbols represent individual samples; bars show the mean. * = $P < 0.05$. **E,** The amount of collagen content in skin sections was quantified using an assay kit (n = 5 samples per group). Symbols represent individual samples; bars show the mean. * = $P < 0.05$.

bleomycin-treated mouse skin. Accordingly, we tried to determine whether IL-20 supplementation could reverse skin fibrosis in SSc.

Bleomycin (300 μg) or control PBS was locally injected into the back of BALB/c mice 6 times per week for 1 month, and at the same time PBS or IL-20 (3.5 μg) was injected once per week (4 times per month) (further information available from the corresponding author). In the absence of bleomycin injection, IL-20 reduced dermal thickness slightly, but the difference was not significant. Bleomycin treatment without IL-20 induced dermal fibrosis with an increased number of thickened collagen bundles (Figure 5B). However, IL-20 reduced the extent of bleomycin-induced skin thickening (Figure 5B). In immunohistochemical staining using paraffin-embedded mouse skin sections, the expression of Fli-1 in fibroblast-like spindle cells was increased by IL-20, while the expression of Smad3 was decreased (Figure 5C),

consistent with in vitro results. We found that reversal of bleomycin-induced dermal thickening by IL-20 was statistically significant (Figure 5D). In addition, the increased amount of collagen induced by bleomycin in skin tissue was also significantly decreased by IL-20 (Figure 5E). Taken together, these results indicate that IL-20 supplementation could attenuate bleomycin-induced skin fibrosis.

DISCUSSION

In the skin, IL-20 is known to induce keratinocyte proliferation, but the effect on dermal fibroblasts has not been investigated. Our study revealed that $\alpha 2$(I) collagen mRNA expression was reduced by IL-20 at the transcriptional level, and that the decrease was mediated by Fli-1 induction in normal dermal fibroblasts. We did not determine the regulatory mechanism of the type I collagen $\alpha 1$ chain in the present study, but there may be similar mechanisms in IL-20–mediated $\alpha 1$(I) collagen down-regulation, because Fli-1 also controls $\alpha 1$(I) collagen expression (33).

There was a significant difference in serum IL-20 levels between patients with scleroderma spectrum disorders and normal subjects. As described above, scleroderma spectrum disorder is a prodromal stage of SSc, and a similar condition was also reported as "limited SSc" by LeRoy and Medsger (42). Because fibrotic change in SSc is usually irreversible, new strategies are needed to diagnose patients as early as possible and to follow them up carefully. For that purpose, the concept of scleroderma spectrum disorder is helpful. Serum IL-20 levels may be useful for differentiating patients with scleroderma spectrum disorders from normal subjects.

Generally, patients with scleroderma spectrum disorders lack a fibrotic response but show prominent clinical symptoms associated with vasculopathy (further information available from the corresponding author). Given that there have been a couple of articles regarding the role of IL-20 in angiogenesis (43,44), decreased serum IL-20 levels in patients with scleroderma spectrum disorders suggests that IL-20 is potentially linked to the pathogenesis of vasculopathy leading to the development of fibrosis. However, as the limitation of this study, scleroderma spectrum disorders potentially include undifferentiated connective tissue diseases developing into collagen diseases other than SSc. Therefore, it is basically impossible to say that all patients with scleroderma spectrum disorders included in this study have an established clinical entity that will develop into SSc. Longitudinal studies of serum IL-20 levels in patients with SSc developed from scleroderma spectrum disorders are needed in the future.

We found that IL-20 expression was decreased in SSc epidermis. We have a hypothetical model of IL-20–mediated tissue fibrosis in SSc (further information available from the corresponding author). Reduction of IL-20 expression in SSc skin may further down-regulation of Fli-1, with subsequent collagen overexpression in SSc fibroblasts; Fli-1 was reported to be constitutively decreased in SSc fibroblasts, probably due to TGFβ signaling (45), and reduction of IL-20 expression may enhance Fli-1 down-regulation. The addition of ectopic IL-20 reduces collagen expression effectively, via Fli-1 recovery and suppression of Smad3 and endoglin. In addition, the epidermis of SSc skin is known to become atrophic, and this may be because of reduced keratinocyte proliferation resulting from decreased IL-20. On the other hand, in psoriasis, IL-20 is thought to be overexpressed in epidermis and to lead to characteristic keratinocyte proliferation and epidermal thickening (13). This may explain why psoriasis skin is protected from dermal fibrosis despite chronic inflammation.

Our model indicates that IL-20 may have therapeutic value for the fibrotic condition of SSc. We were able to inhibit bleomycin-induced fibrosis by using IL-20 supplementation in the mouse model. To date, steroids, cyclophosphamide, and methotrexate are considered the first-choice drugs for treating the severe skin fibrosis of SSc (46,47). However, these conventional treatments usually have limited effects. Furthermore, these treatments are often accompanied by various significant adverse effects (48). Clarifying the mechanism by which IL-20 regulates tissue fibrosis in SSc skin may lead to a better understanding of this disease and to new therapeutic approaches. However, our study has other limitations involving potential contradiction of our in vivo results with our in vitro results. For example, further studies are needed to examine the function and expression pattern of IL-20R in murine dermal fibroblasts. Similarly, the data showing that the inhibitory effect of IL-20 on collagen was blocked by Fli-1 siRNA in vitro should be confirmed in vivo (i.e., the effect of IL-20 on bleomycin-induced dermal fibrosis in Fli-1–knockout mice should be determined).

AUTHOR CONTRIBUTIONS

All authors were involved in drafting the article or revising it critically for important intellectual content, and all authors approved the final version to be published. Dr. Jinnin had full access to all of the data in the study and takes responsibility for the integrity of the data and the accuracy of the data analysis.

Study conception and design. Jinnin, Asano, Trojanowska, Fukushima, Ihn.

Acquisition of data. Kudo, Nakayama, Inoue.
Analysis and interpretation of data. Kudo, Jinnin, Honda, Kajihara, Makino.

REFERENCES

1. Uitto J, Kouba D. Cytokine modulation of extracellular matrix gene expression: relevance to fibrotic skin diseases. J Dermatol Sci 2000;24:60–9.
2. Trojanowska M, LeRoy EC, Eckes B, Krieg T. Pathogenesis of fibrosis: type I collagen and the skin. J Mol Med (Berl) 1998;76: 266–74.
3. Varga J, Abraham D. Systemic sclerosis: a prototypic multisystem fibrotic disorder. J Clin Invest 2007;117:557–67.
4. Gabrielli A, Avvedimento EV, Krieg T. Scleroderma. N Engl J Med 2009;360:1989–2003.
5. Ihn H, Yamane K, Kubo M, Tamaki K. Blockade of endogenous transforming growth factor β signaling prevents up-regulated collagen synthesis in scleroderma fibroblasts: association with increased expression of transforming growth factor β receptors. Arthritis Rheum 2001;44:474–80.
6. Asano Y, Ihn H, Yamane K, Kubo M, Tamaki K. Impaired Smad7-Smurf-mediated negative regulation of TGF-β signaling in scleroderma fibroblasts. J Clin Invest 2004;113:253–64.
7. Takehara K. Hypothesis: pathogenesis of systemic sclerosis. J Rheumatol 2003;30:755–9.
8. Overbeek MJ, Boonstra A, Voskuyl AE, Vonk MC, Vonk-Noordegraaf A, van Berkel MP, et al. Platelet-derived growth factor receptor-β and epidermal growth factor receptor in pulmonary vasculature of systemic sclerosis-associated pulmonary arterial hypertension versus idiopathic pulmonary arterial hypertension and pulmonary veno-occlusive disease: a case-control study. Arthritis Res Ther 2011;13:R61.
9. Brissett M, Veraldi KL, Pilewski JM, Medsger TA Jr, Feghali-Bostwick CA. Localized expression of tenascin in systemic sclerosis–associated pulmonary fibrosis and its regulation by insulin-like growth factor binding protein 3. Arthritis Rheum 2012;64: 272–80.
10. Kawaguchi Y. IL-1α gene expression and protein production by fibroblasts from patients with systemic sclerosis. Clin Exp Immunol 1994;97:445–50.
11. Feghali CA, Bost KL, Boulware DW, Levy LS. Mechanisms of pathogenesis in scleroderma. I. Overproduction of interleukin 6 by fibroblasts cultured from affected skin sites of patients with scleroderma. J Rheumatol 1992;19:1207–11.
12. Makino T, Fukushima S, Wakasugi S, Ihn H. Decreased serum IL-7 levels in patients with systemic sclerosis. Clin Exp Rheumatol 2009;27:68–9.
13. Blumberg H, Conklin D, Xu WF, Grossmann A, Brender T, Carollo S, et al. Interleukin 20: discovery, receptor identification, and role in epidermal function. Cell 2001;104:9–19.
14. Wegenka UM. IL-20: biological functions mediated through two types of receptor complexes. Cytokine Growth Factor Rev 2010; 21:353–63.
15. Gallagher G, Dickensheets H, Eskdale J, Izotova LS, Mirochnitchenko OV, Peat JD, et al. Cloning, expression and initial characterisation of interleukin-19 (IL-19), a novel homologue of human interleukin-10 (IL-10). Genes Immun 2000;1:442–50.
16. Liao YC, Liang WG, Chen FW, Hsu JH, Yang JJ, Chang MS. IL-19 induces production of IL-6 and TNF-α and results in cell apoptosis through TNF-α. J Immunol 2002;169:4288–97.
17. Jiang H, Lin JJ, Su ZZ, Goldstein NI, Fisher PB. Subtraction hybridization identifies a novel melanoma differentiation associated gene, mda-7, modulated during human melanoma differentiation, growth and progression. Oncogene 1995;11:2477–86.
18. Hsu YH, Li HH, Hsieh MY, Liu MF, Huang KY, Chin LS, et al. Function of interleukin-20 as a proinflammatory molecule in rheumatoid and experimental arthritis. Arthritis Rheum 2006;54: 2722–33.
19. Li HH, Cheng HH, Sun KH, Wei CC, Li CF, Chen WC, et al. Interleukin-20 targets renal mesangial cells and is associated with lupus nephritis. Clin Immunol 2008;129:277–85.
20. Wei CC, Chang MS. A novel transcript of mouse interleukin-20 receptor acts on glomerular mesangial cells as an aggravating factor in lupus nephritis. Genes Immun 2008;9:668–79.
21. Sa SM, Valdez PA, Wu J, Jung K, Zhong F, Hall L, et al. The effects of IL-20 subfamily cytokines on reconstituted human epidermis suggest potential roles in cutaneous innate defense and pathogenic adaptive immunity in psoriasis. J Immunol 2007;178: 2229–40.
22. Subcommittee for Scleroderma Criteria of the American Rheumatism Association Diagnostic and Therapeutic Criteria Committee. Preliminary criteria for the classification of systemic sclerosis (scleroderma). Arthritis Rheum 1980;23:581–90.
23. Maricq HR, McGregor AR, Diat F, Smith EA, Maxwell DB, LeRoy EC, et al. Major clinical diagnoses found among patients with Raynaud phenomenon from the general population. J Rheumatol 1990;17:1171–6.
24. Maricq HR, Weinrich MC, Keil JE, Smith EA, Harper FE, Nussbaum AI, et al. Prevalence of scleroderma spectrum disorders in the general population of South Carolina. Arthritis Rheum 1989;32:998–1006.
25. Ihn H, Sato S, Tamaki T, Soma Y, Tsuchida T, Ishibashi Y, et al. Clinical evaluation of scleroderma spectrum disorders using a points system. Arch Dermatol Res 1992;284:391–5.
26. Honda N, Jinnin M, Kira-Etoh T, Makino K, Kajihara I, Makino T, et al. miR-150 down-regulation contributes to the constitutive type I collagen overexpression in scleroderma dermal fibroblasts via the induction of integrin β3. Am J Pathol 2013;182:206–16.
27. Jinnin M, Makino T, Kajihara I, Honda N, Makino K, Ogata A, et al. Serum levels of soluble vascular endothelial growth factor receptor-2 in patients with systemic sclerosis. Br J Dermatol 2010;162:751–8.
28. Noda S, Asano Y, Akamata K, Aozasa N, Taniguchi T, Takahashi T, et al. Constitutive activation of c-Abl/protein kinase C-δ/Fli1 pathway in dermal fibroblasts derived from patients with localized scleroderma. Br J Dermatol 2012;167:1098–105.
29. Asano Y, Trojanowska M. Phosphorylation of Fli1 at threonine 312 by protein kinase C δ promotes its interaction with p300/CREB-binding protein-associated factor and subsequent acetylation in response to transforming growth factor β. Mol Cell Biol 2009;29:1882–94.
30. Ihn H, Ohnishi K, Tamaki T, LeRoy EC, Trojanowska M. Transcriptional regulation of the human α2(I) collagen gene: combined action of upstream stimulatory and inhibitory cis-acting elements. J Biol Chem 1996;271:26717–23.
31. Filippova M, Song H, Connolly JL, Dermody TS, Duerksen-Hughes PJ. The human papillomavirus 16 E6 protein binds to tumor necrosis factor (TNF) R1 and protects cells from TNF-induced apoptosis. J Biol Chem 2002;277:21730–9.
32. Wolk K, Witte E, Warszawska K, Schulze-Tanzil G, Witte K, Philipp S, et al. The Th17 cytokine IL-22 induces IL-20 production in keratinocytes: a novel immunological cascade with potential relevance in psoriasis. Eur J Immunol 2009;39:3570–81.
33. Yamamoto T, Takagawa S, Katayama I, Yamazaki K, Hamazaki Y, Shinkai H, et al. Animal model of sclerotic skin. I. Local injections of bleomycin induce sclerotic skin mimicking scleroderma. J Invest Dermatol 1999;112:456–62.
34. Tanaka C, Fujimoto M, Hamaguchi Y, Sato S, Takehara K, Hasegawa M. Inducible costimulator ligand regulates bleomycin-induced lung and skin fibrosis in a mouse model independently of the inducible costimulator/inducible costimulator ligand pathway. Arthritis Rheum 2010;62:1723–32.
35. Marotta M, Martino G. Sensitive spectrophotometric method for the quantitative estimation of collagen. Anal Biochem 1985;150: 86–90.

36. Czuwara-Ladykowska J, Shirasaki F, Jackers P, Watson DK, Trojanowska M. Fli-1 inhibits collagen type I production in dermal fibroblasts via an Sp1-dependent pathway. J Biol Chem 2001;276: 20839–48.
37. Czuwara-Ladykowska J, Sementchenko VI, Watson DK, Trojanowska M. Ets1 is an effector of the transforming growth factor β (TGF-β) signaling pathway and an antagonist of the profibrotic effects of TGF-β. J Biol Chem 2002;277:20399–408.
38. Jinnin M, Ihn H, Yamane K, Mimura Y, Asano Y, Tamaki K. α2(I) collagen gene regulation by protein kinase C signaling in human dermal fibroblasts. Nucleic Acids Res 2005;33:1337–51.
39. Asano Y, Ihn H, Yamane K, Jinnin M, Mimura Y, Tamaki K. Phosphatidylinositol 3-kinase is involved in α2(I) collagen gene expression in normal and scleroderma fibroblasts. J Immunol 2004;172:7123–35.
40. Morris E, Chrobak I, Bujor A, Hant F, Mummery C, Ten Dijke P, et al. Endoglin promotes TGF-β/Smad1 signaling in scleroderma fibroblasts. J Cell Physiol 2011;226:3340–8.
41. Clements P, Lachenbruch P, Seibold J, White B, Weiner S, Martin R, et al. Inter and intraobserver variability of total skin thickness score (modified Rodnan TSS) in systemic sclerosis. J Rheumatol 1995;22:1281–5.
42. LeRoy EC, Medsger TA Jr. Criteria for the classification of early systemic sclerosis. J Rheumatol 2001;28:1573–6.
43. Hsieh MY, Chen WY, Jiang MJ, Cheng BC, Huang TY, Chang MS. Interleukin-20 promotes angiogenesis in a direct and indirect manner. Genes Immun 2006;7:234–42.
44. Heuze-Vourc'h N, Liu M, Dalwadi H, Baratelli FE, Zhu L, Goodglick L, et al. IL-20, an anti-angiogenic cytokine that inhibits COX-2 expression. Biochem Biophys Res Commun 2005;333: 470–5.
45. Asano Y, Markiewicz M, Kubo M, Szalai G, Watson DK, Trojanowska M. Transcription factor Fli1 regulates collagen fibrillogenesis in mouse skin. Mol Cell Biol 2009;29:425–34.
46. Apras S, Ertenli I, Ozbalkan Z, Kiraz S, Ozturk MA, Haznedaroglu IC, et al. Effects of oral cyclophosphamide and prednisolone therapy on the endothelial functions and clinical findings in patients with early diffuse systemic sclerosis. Arthritis Rheum 2003;48:2256–61.
47. Pope JE, Bellamy N, Seibold JR, Baron M, Ellman M, Carette S, et al. A randomized, controlled trial of methotrexate versus placebo in early diffuse scleroderma. Arthritis Rheum 2001;44: 1351–8.
48. Haustein UF. Systemic sclerosis-scleroderma. Dermatol Online J 2002;8:3.

THE JOURNAL OF DERMATOLOGY

doi: 10.1111/1346-8138.12495

Journal of Dermatology 2014; **41**: 533–535

CONCISE COMMUNICATION

Successful use of intravenous cyclophosphamide pulse therapy for interstitial lung disease in a patient with systemic sclerosis on hemodialysis

Takehiro TAKAHASHI,[1] Yoshihide ASANO,[1] Ryo SUNAGA,[1] Yohei ICHIMURA,[1] Takashi TANIGUCHI,[1] Mizuho YAMAMOTO,[1] Zenshiro TAMAKI,[1] Tomonori TAKEKOSHI,[1] Hiroshi MITSUI,[1] Makoto SUGAYA,[1] Takamoto OHSE,[2] Shinichi SATO[1]

[1]*Department of Dermatology, and* [2]*Divison of Nephrology and Endocrinology, University of Tokyo Graduate School of Medicine, Tokyo, Japan*

ABSTRACT

Interstitial lung disease and scleroderma renal crisis are major complications of systemic sclerosis, which occasionally coexist in patients with the diffuse cutaneous subtype. We herein report a case of diffuse cutaneous systemic sclerosis under hemodialysis due to a previous history of scleroderma renal crisis, whose interstitial lung disease was effectively and safely treated with a half dose of i.v. cyclophosphamide pulse. The dose of cyclophosphamide and the timing of hemodialysis leading to efficacy and low toxicity are discussed.

Key words: hemodialysis, interstitial lung disease, intravenous cyclophosphamide pulse, scleroderma renal crisis, systemic sclerosis.

INTRODUCTION

Systemic sclerosis (SSc) is a multisystem autoimmune disease characterized by vasculopathy and fibrosis of the skin and certain internal organs. Interstitial lung disease (ILD) is a major visceral involvement determining the prognosis of SSc, especially diffuse cutaneous SSc (dcSSc), as well as pulmonary arterial hypertension.[1] Thus far, the combination therapy of prednisone with intravenous cyclophosphamide pulse (IVCY) is the first-line treatment and has been widely used against ILD associated with SSc.[2] Scleroderma renal crisis (SRC) is another important vascular complication mainly observed in patients with early dcSSc. After the emergence of angiotensin-converting enzyme inhibitors, the prognosis of SRC has been dramatically improved,[3] but the delayed diagnosis and treatment often results in induction of hemodialysis (HD). Because SRC mostly occurs in patients with early progressive dcSSc, this complication often coexists with ILD. Therefore, it appears not to be rare to administrate IVCY to SSc-ILD patients under HD due to the previous history of SRC. However, to the best of our knowledge, there has been no report regarding IVCY therapy on SSc-ILD patients under HD. We herein report a case of SSc-ILD under HD due to a past history of SRC, who was successfully treated with a half dose of IVCY. We also discuss the dose of cyclophosphamide and the timing of HD leading to efficacy and low toxicity of IVCY.

CASE REPORT

A 63-year-old woman without any remarkable past medical history was referred to our hospital in November 2009 for the treatment of rapidly deteriorating hypertension and renal function. She had noticed Raynaud's phenomenon since winter 2000 and swelling of her fingers since winter 2006. From spring 2008, she had experienced dyspnea during exercise. In November 2009, she suddenly suffered from severe dyspnea. She was admitted to the emergency department of the nearby hospital and then referred to our hospital. On examination, prominent edema and skin thickening spread all over the extremities. Her autoantibody screen revealed a positive antinuclear antibody with a titer of 1:320 homogeneous and speckled pattern, corresponding to anti-topoisomerase I antibody. Antineutrophil cytoplasmic antibodies and rheumatoid factor were negative. Complement levels and hepatic profiles were within normal limits, but her renal profile revealed markedly elevated serum creatinine level (7.72 mg/dL). Erythrocyte sedimentation rate (114 mm/h) and C-reactive protein (2.22 mg/dL) were elevated. A skin biopsy from the right forearm showed diffuse dermal fibrosis and a slight lymphocytic perivascular infiltrate. High-resolution computed tomography (HRCT) scan of the lungs revealed early bibasilar interstitial changes (Fig. 1a). A diagnosis of SSc with ongoing renal crisis was made, and enalapril and nicardipine were introduced. However,

Correspondence: Yoshihide Asano, M.D., Ph.D., Department of Dermatology, University of Tokyo Graduate School of Medicine, 7-3-1 Hongo, Bunkyo-ku, Tokyo 113-8655, Japan. Email: yasano-tky@umin.ac.jp

Received 25 February 2014; accepted 13 March 2014.

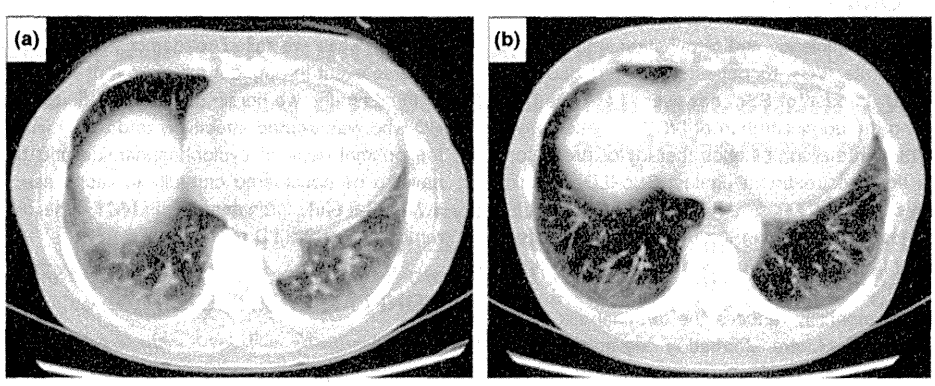

Figure 1. High-resolution computed tomography (HRCT) scan before and after intravenous cyclophosphamide pulse (IVCY). (a) HRCT in November 2009. Before IVCY, the lungs revealed early bibasilar interstitial changes. (b) HRCT in October 2010. After IVCY, the image revealed a remarkable resolution of ILD.

the renal dysfunction was progressive and HD was introduced. After that, the patient became stable and was discharged.

In July 2010, she became increasingly dyspneic and the dry cough worsened. A blood test revealed increasing KL-6 and SP-D values (Fig. 2). The patient was clinically quite unwell with evidence of progressive worsening of ILD. Under close communication with nephrologists, we decided to treat this patient with IVCY to halt the deterioration. Before the therapy, she had been treated with HD for 3 h, three times a week. At the introduction of the therapy, the patient was admitted and the schedule was changed to HD twice a week (Tuesday and Friday) because the pre-dialysis serum creatinine had been

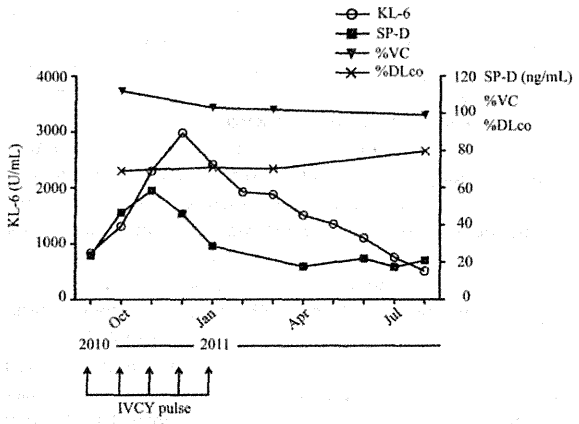

Figure 2. Time course of serum markers of interstitial lung disease, KL-6 and SP-D, with vital capacity (%VC) and diffusing capacity for carbon monoxide (%DLco) of pulmonary function tests. Left Y-axis for serum KL-6 values and right Y-axis for serum SP-D values, %VC and %DLco of pulmonary function tests. Although %VC and %DLco did not show remarkable changes during or after intravenous cyclophosphamide pulses, SP-D values started to decline after the third pulse, followed by the decline of KL-6 values.

improving. An intermediate dose of prednisone (20 mg/day) was started and the first IVCY was infused on Wednesday, the day after the HD, to avoid the clearance of cyclophosphamide by HD. Considering the potential increased risk for adverse events due to prolonged drug exposure caused by decreased clearance, the initial dose of 370 mg, a half dose of 500 mg/m^2 body surface area commonly administrated, was given without hydration infusion, which is routinely done for IVCY against SSc-ILD at our facility to prevent interstitial cystitis. Thus, the patient was started on a regime of monthly infusions with a half dose of IVCY for 5 months.

There was a good response to induction therapy with IVCY and no remarkable adverse event was noticed. The patient felt clinically better and did not complain of dyspnea or dry cough after the first two pulses. A HRCT scan of the lungs done in October 2010, post-induction of remission therapy with IVCY, revealed significant improvement of ILD (Fig. 1b). Even though the pulmonary function test results did not show similar improvements, the patient was symptomatically (i.e. dyspnea and dry cough) quite well. Markers of interstitial lung disease, KL-6 and SP-D, kept increasing during the first three pulses, but SP-D started to decline after the third pulse, followed by the decrease in KL-6 value (Fig. 2). The HRCT lung scans done in January 2011 revealed minimal early bibasilar interstitial and bronchiectatic changes (data not shown). There was no evidence of progression of fibrosis or ground glass appearance to suggest active ILD. We seemed to have been successful in preventing further progression of ILD without any significant adverse event. All clinical and biochemical parameters were normal. The patient is undergoing regular reviews to watch out for relapse of ILD or worsening of systemic symptoms.

DISCUSSION

Intravenous cyclophosphamide pulse is an established treatment for various autoimmune inflammatory diseases, including systemic lupus erythematosus (SLE) and systemic vasculitis. Given that patients with SLE and systemic vasculitis, such as

granulomatosis with polyangiitis and microscopic polyangiitis, often manifest renal insufficiency and terminal renal failure, it is not rare to administrate IVCY to patients with reduced renal function and on HD. In case of SSc, however, there has been no report regarding the administration of IVCY to patients with ILD under HD although the combination therapy of prednisone and IVCY is the first-line treatment against SSc-ILD, in which SRC occasionally coexists.

The important factor determining the efficacy and toxicity of IVCY is the concentration of its effective metabolite, phosphoramide mustard, which has the most ultimate alkylating property.[4,5] Prednisone potentially reduces the terminal elimination half-life and increases the biotransformation rate of cyclophosphamide,[6] which is a theoretical reason why the combination therapy of IVCY with prednisone is recommended to obtain its maximal clinical efficacy. As for the impact of reduced renal function on the pharmacokinetics and toxicity profile of cyclophosphamide, it is still controversial whether or not dose adjustment is recommended. Some studies showed no influence of renal dysfunction on the pharmacokinetics and toxicity of cyclophosphamide,[7–9] while others reported the decrease in clearance of both cyclophosphamide and its alkylating metabolites resulting in an enhanced toxicity.[10–12] Following these studies and others reporting the pharmacokinetics of cyclophosphamide in patients on HD,[13,14] Haubitz *et al.*[15] demonstrated the detailed data regarding the impact of HD on the pharmacokinetics of cyclophosphamide in 15 patients with autoimmune diseases treated with IVCY. According to their results, the clearance of cyclophosphamide is decreased in patients with reduced renal function, thereby resulting in an increased systemic drug exposure. Furthermore, cyclophosphamide is effectively eliminated from systemic circulation by HD, while the area under the curve of cyclophosphamide is almost identical to that of healthy controls when 3-h HD is carried out 7 h after the administration of IVCY. Based on these data, the authors concluded that dose reduction of 20–30%, depending on the degree of renal insufficiency, is suggested to prevent potential therapy-related toxicity and that dialysis should not be initiated earlier than 12 h after IVCY, which would prevent drug removal in the early distribution phase but would still correct for the prolonged terminal elimination phase.[15]

In our case, based on the previous data, we decided to administrate a half dose of IVCY to carefully avoid the potential toxicity while conducting HD 48 h after the administration in order to obtain its maximal clinical effect on SSc-ILD. Given that circulating cyclophosphamide concentration is decreased below the biologically active levels 24 h after the administration,[15] it was assumed that HD did not weaken the effect of IVCY in the present case. In spite of the modest dose, her subjective symptoms significantly improved together with the marked decrease in ground glass opacity on pulmonary HRCT images, while we failed to detect any clinical and laboratory adverse event throughout the course of whole IVCY.

In summary, we herein reported the first case of SSc-ILD on HD who was treated effectively and safely with IVCY. Although the optimal dose of cyclophosphamide and the timing of HD have to be considered carefully in each case, we need to be aware that early intervention with IVCY is helpful in induction of remission in SSc-ILD even if on HD.

CONFLICT OF INTEREST: None.

REFERENCES

1 Bussone G, Mouthon L. Interstitial lung disease in systemic sclerosis. *Autoimmun Rev* 2011; **10**: 248–255.
2 Mouthon L, Berezne A, Guillevin L, Valeyre D. Therapeutic options for systemic sclerosis related interstitial lung diseases. *Respir Med* 2010; **104**(Suppl 1): S59–S69.
3 Steen VD, Medsger TA Jr. Severe organ involvement in systemic sclerosis with diffuse scleroderma. *Arthritis Rheum* 2000; **43**: 2437–2444.
4 Struck RF, Kirk MC, Witt MH, Laster WR. Isolation and mass spectral identification of blood metabolites of cyclophosphamide: evidence for phosphoramide mustard as the biologically active metabolite. *Biomed Mass Spectrom* 1975; **2**: 46–52.
5 Colvin M, Brundrett RB, Kan MN, Jardine I, Fenselau C. Alkylating properties of phosphoramide mustard. *Cancer Res* 1976; **36**: 1121–1126.
6 Faber OK, Mouridsen HT, Skovsted L. The biotransformation of cyclophosphamide in man: influence of prednisone. *Acta Pharmacol Toxicol (Copenh)* 1974; **35**: 195–200.
7 Grochow LB, Colvin M. Clinical pharmacokinetics of cyclophosphamide. *Clin Pharmacokinet* 1979; **4**: 380–394.
8 Moore MJ. Clinical pharmacokinetics of cyclophosphamide. *Clin Pharmacokinet* 1991; **20**: 194–208.
9 Bramwell V, Calvert RT, Edwards G, Scarffe H, Crowther D. The disposition of cyclophosphamide in a group of myeloma patients. *Cancer Chemother Pharmacol* 1979; **3**: 253–259.
10 Bagley CM, Bostick FW, DeVita VT. Clinical pharmacology of cyclophosphamide. *Cancer Res* 1973; **33**: 226–233.
11 Juma FD, Rogers HJ, Trounce JR. Effect of renal insufficiency on the pharmacokinetics of cyclophosphamide and some of its metabolites. *Eur J Clin Pharmacol* 1981; **19**: 443–451.
12 Mouridsen HT, Jacobsen E. Pharmacokinetics of cyclophosphamide in renal failure. *Acta Pharmacol Toxicol (Copenh)* 1975; **36**: 409–414.
13 Wang LH, Lee CS, Majeske BL, Marbury TC. Clearance and recovery calculations in hemodialysis: application to plasma, red blood cells, and dialysate measurements for cyclophosphamide. *Clin Pharmacol Ther* 1981; **29**: 365–372.
14 Milsted RA, Jarman M. Haemodialysis during cyclophosphamide treatment. *Br Med J* 1978; **1**: 820–821.
15 Haubitz M, Bohnenstengel F, Brunkhorst R, Schwab M, Hofmann U, Busse D. Cyclophosphamide pharmacokinetics and dose requirements in patients with renal insufficiency. *Kidney Int* 2002; **61**: 1495–1501.

THE JOURNAL OF DERMATOLOGY

doi: 10.1111/1346-8138.12461

Journal of Dermatology 2014; **41**: 418–420

CONCISE COMMUNICATION

Successful experience of rituximab therapy for systemic sclerosis-associated interstitial lung disease with concomitant systemic lupus erythematosus

Hayakazu SUMIDA, Yoshihide ASANO, Zenshiro TAMAKI, Naohiko AOZASA, Takashi TANIGUCHI, Takehiro TAKAHASHI, Tetsuo TOYAMA, Yohei ICHIMURA, Shinji NODA, Kaname AKAMATA, Miki MIYAZAKI, Yoshihiro KUWANO, Koichi YANABA, Shinichi SATO

Department of Dermatology, Faculty of Medicine, The University of Tokyo, Tokyo, Japan

ABSTRACT

Previous studies have demonstrated that B cells play critical roles in autoimmune disorders including systemic sclerosis (SSc) and systemic lupus erythematosus (SLE). However, the effectiveness of rituximab (RTX), a chimeric anti-CD20 antibody, for SSc-associated interstitial lung disease (ILD) or SLE disease activity remains controversial. We herein report an SSc patient with severely progressed ILD and concomitant SLE treated by two cycles of RTX at baseline and half a year later. This treatment improved ILD and SLE activities, along with reduction of dermal sclerosis and serum anti-topoisomerase I antibody levels. In addition, our detailed time-course data indicate that half a year may be appropriate as an interval between each cycle of RTX therapy aimed at SSc-associated ILD or SLE. Overall, the current report could pave the way to establish RTX as a disease-modifying drug for patients with SSc and/or SLE showing resistance to other already approved medications.

Key words: **B cells, interstitial lung disease, rituximab, systemic lupus erythematosus, systemic sclerosis.**

INTRODUCTION

Systemic sclerosis (SSc) is a chronic connective tissue disorder characterized by injury to vascular walls and following fibrosis in certain organs such as skin and lung. SSc-associated interstitial lung disease (SSc-ILD) is one of the main causes of death in SSc patients.[1] Although most drugs tested so far have shown poor or modest results, cyclophosphamide has shown statistically significant but temporal efficacy for the treatment of SSc-ILD.[2] Therefore, development of additional therapeutic options for SSc-ILD has been desired. Although the pathogenesis of SSc remains unknown, several lines of evidence in SSc patients and animal models indicate a potential role of B cells in SSc.[3,4] Rituximab (RTX) is a chimeric antibody binding to the transmembrane CD20 receptor on the surface of B lymphocytes, which causes B-cell depletion and has been successfully used in the treatment of a variety of autoimmune diseases. Recent studies revealed possible clinical effects of RTX therapy on SSc[5–10] as well as systemic lupus erythematosus (SLE).[11,12] As for the effect of RTX on ILD secondary to SSc, some reports demonstrated that RTX significantly improved lung function,[8–10] while other studies described that pulmonary function tests remained stable during their follow up after RTX therapy.[5–7] Therefore, it turns out that the validity of RTX therapy for lung fibrosis in SSc remains controversial, as is the case for SLE activity.[13] We report herein a patient with long-standing diffuse cutaneous SSc (dcSSc) and concomitant SLE, who received two cycles of RTX at baseline and half a year later.

CASE REPORT

A 48-year-old Japanese woman had suffered from severe peripheral circulatory disturbances with digital ulcers from 1994 (aged 30 years). She was diagnosed with dcSSc and concomitant SLE in 2004 (aged 40 years). Antibodies to topoisomerase I (Topo I) and U1 ribonucleoprotein were detected in her laboratory data. In 2004, ILD was evident with reduced forced vital capacity (FVC) and diffusing capacity for carbon monoxide (DLco) values to 84% and 55% of predicted, respectively. Furthermore, a slight elevation of serum biomarkers for ILD such as Krebs von den Lungen-6 (KL-6; cut-off level, 500 U/mL) and surfactant protein D (SP-D; cut-off level, 110 ng/mL) was found (526 U/mL and 116 ng/mL, respectively). Subsequently, she gradually developed dyspnea on exertion (New York Heart Association class III) along with the decline of lung function tests to 59% and 31% for FVC and DLco, respectively, in 2009. Concurrently, reticular and honeycomb patterns on computed tomography (CT) scans were deteriorated and serum levels of

Correspondence: Yoshihide Asano, M.D., Ph.D., Department of Dermatology, Faculty of Medicine, The University of Tokyo, 7-3-1 Hongo, Bunkyo-ku, Tokyo 113-8655, Japan. Email: yasano-tky@umin.ac.jp

Received 26 December 2013; accepted 5 February 2014.

KL-6 and SP-D were elevated to 1642 U/mL and 136 ng/mL, respectively (Fig. 1). In an attempt to stop the progression of ILD, she received i.v. cyclophosphamide (IVCY) pulse therapy (a test dose of 350 mg/m^2 at the first month followed by four cycles of monthly IVCY at a dose of 500 mg/m^2) with moderate dose of prednisolone (30 mg/day) in 2010 with improvement of her respiratory symptoms, biomarkers (1246 U/mL and 76 ng/mL for KL-6 and SP-D, respectively; Fig. 1) and lung function tests (66% and 34% for FVC and DLco, respectively; Fig. 1). Unfortunately, she could not continue IVCY pulse therapy due to her allergic reaction to cyclophosphamide such as fatigue and fever. Therefore, she was followed by the treatment with mizoribine (300 mg/day). However, there was an increased frequency of dry cough accompanied by increased biomarkers (1621 U/mL and 107 ng/mL for KL-6 and SP-D, respectively; Fig. 1) and deterioration in respiratory function (57% and 31% for FVC and DLco, respectively; Fig. 1) in 2011. What is worse was that she showed the expansion in the area of ground glass opacities and honeycomb lung on CT images. In consideration of the exacerbation of her ILD, we planned an independent clinical study of RTX for the treatment of ILD associated with SSc. The Medical Ethical Committee of The University of Tokyo approved the study protocol, which fulfilled the Declaration of Helsinki requirements. A written informed consent was obtained from this patient. She received two cycles of RTX at baseline and 6 months later. Each cycle consisted of four weekly RTX infusions at the dose of 375 mg/m^2 according to a previous report.[8] She noticed the improvement of her respiratory symptoms gradually after the first cycle. CT scan images revealed the reduction in the area of ground glass opacities in lungs with the recovery of FVC and DLco to 62% and 41%, respectively (Fig. 1b). Moreover, the serum levels of KL-6 and SP-D were dramatically decreased to 763 U/mL and 57 ng/mL, respectively (Fig. 1). In addition, reduction of modified Rodnan skin scores was observed from 12 to 8 after two cycles of RTX therapy. Furthermore, the titer levels of serum anti-Topo I antibodies showed a gradual decline after the RTX administration (Fig. 2), along with the decrease in serum immunoglobulin G levels. Of note, successful depletion of B cells was confirmed by flow cytometric analysis of peripheral blood leukocytes during the RTX treatment (Fig. 2). In regards to her SLE activity, she had shown serological abnormalities such as high levels of anti-dsDNA antibodies and decrease in serum complement (CH50, C3 and C4) levels despite the treatment with prednisolone (15 mg/day) for a long time before the treatment with IVCY and RTX. Serum levels of anti-dsDNA antibodies, CH50, C3 and C4 were all improved to the normal levels by the administration of IVCY and RTX (Fig. 1), indicating the effectiveness of RTX for SLE. In consideration of RTX-induced impaired immunity, patient safety was ensured during the course of this study by periodic laboratory monitoring, such as β-D-glucan and cytomegalovirus antigen levels in the blood.

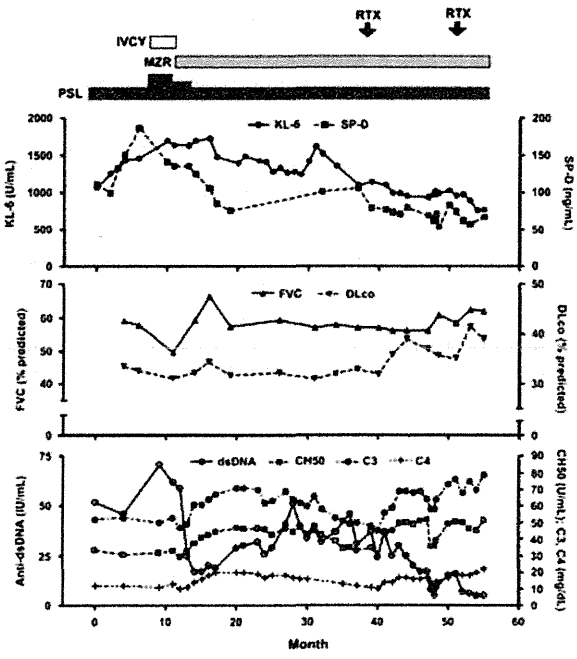

Figure 1. Time course of treatment and parameters in a patient with systemic sclerosis (SSc) and systemic lupus erythematosus (SLE). Upper panel: serum levels of Krebs von den Lungen-6 (KL-6) and surfactant protein D (SP-D). Middle panel: results of forced vital capacity (FVC) (% predicted) and diffusing capacity for carbon monoxide (DLco) (% predicted) from lung function tests. Bottom panel: serum levels of anti-dsDNA antibodies, CH50, C3 and C4. MZR, mizoribine; IVCY, i.v. cyclophosphamide; PSL, prednisolone.

DISCUSSION

In this case, the treatment with RTX dramatically improved ILD-related serum biomarkers, lung function tests parameters and subjective respiratory symptoms. As described in the Introduction section, the validity of RTX for ILD in SSc patients remains controversial. Therefore, this case provides the additional evidence needed to answer this question. Given the

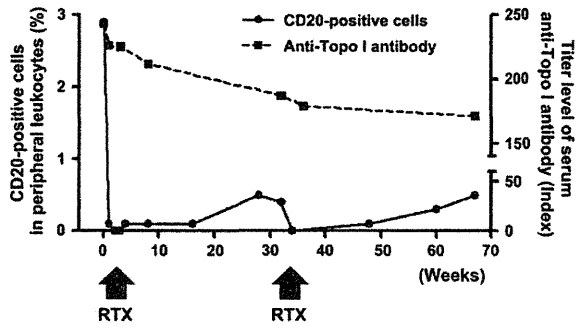

Figure 2. Successful depletion of peripheral CD20-positive leukocytes, followed by gradual decrease in serum titer levels of anti-topoisomerase I (Topo I) antibodies, after rituximab (RTX) administrations.

limited duration of effect after drug discontinuation[14] and toxicity according to long-term use in cyclophosphamide therapy, RTX may be a viable option for patients with SSc-ILD, who are not able to be treated with or resistant to cyclophosphamide. In addition, our data indicated a possible contribution of RTX to the decrease in serum titer levels of anti-Topo I antibodies. Considering that the titers are related to clinical severity of SSc,[15] RTX would ameliorate not only ILD activity but also other various SSc-associated symptoms like skin sclerosis.

There have been a wide variety of protocols for RTX therapy in terms of dose for one treatment, frequency of administration or intervals of each cycle. Especially, further inspections have been required for the RTX treatment aimed at SSc-ILD. At least in the patient described here, improving trends of ILD-associated parameters such as KL-6, SP-D, FVC and DLco were attenuated approximately half a year after the first and second cycles of RTX therapy (4 weekly RTX infusions at the dose of 375 mg/m^2), as is the case in SLE activity parameters (Fig. 1). Of note, the percentage of CD20-positive leukocytes began to increase at similar timing (Fig. 2). Therefore, appropriate intervals of each cycle may be half a year in the RTX treatment for ILD secondary to SSc.

To our best knowledge, this is the first case report of successful RTX treatment in an SSc patient overlapped with SLE. In addition, detailed time-course data of parameters regarding ILD and serum titer levels of anti-Topo I antibodies after the RTX injection have never been documented. Overall, our case report will pave the way for future development of RTX as a disease-modifying drug for SSc-ILD as well as SLE activities.

CONFLICT OF INTEREST: None.

REFERENCES

1 Asano Y. Future treatments in systemic sclerosis. *J Dermatol* 2010; **37**: 54–70.
2 Tashkin DP, Elashoff R, Clements PJ *et al.* Cyclophosphamide versus placebo in scleroderma lung disease. *N Engl J Med* 2006; **354**: 2655–2666.
3 Sato S, Hasegawa M, Fujimoto M, Tedder TF, Takehara K. Quantitative genetic variation in CD19 expression correlates with autoimmunity. *J Immunol* 2000; **165**: 6635–6643.
4 Saito E, Fujimoto M, Hasegawa M *et al.* CD19-dependent B lymphocyte signaling thresholds influence skin fibrosis and autoimmunity in the tight-skin mouse. *J Clin Invest* 2002; **109**: 1453–1462.
5 Smith V, Van Praet JT, Vandooren B *et al.* Rituximab in diffuse cutaneous systemic sclerosis: an open-label clinical and histopathological study. *Ann Rheum Dis* 2010; **69**: 193–197.
6 Lafyatis R, Kissin E, York M *et al.* B cell depletion with rituximab in patients with diffuse cutaneous systemic sclerosis. *Arthritis Rheum* 2009; **60**: 578–583.
7 Bosello S, De Santis M, Lama G *et al.* B cell depletion in diffuse progressive systemic sclerosis: safety, skin score modification and IL-6 modulation in an up to thirty-six months follow-up open-label trial. *Arthritis Res Ther* 2010; **12**: R54.
8 Daoussis D, Liossis SN, Tsamandas AC *et al.* Experience with rituximab in scleroderma: results from a 1-year, proof-of-principle study. *Rheumatology (Oxford)* 2010; **49**: 271–280.
9 Yoo WH. Successful treatment of steroid and cyclophosphamide-resistant diffuse scleroderma-associated interstitial lung disease with rituximab. *Rheumatol Int* 2012; **32**: 795–798.
10 Daoussis D, Liossis SN, Tsamandas AC *et al.* Effect of long-term treatment with rituximab on pulmonary function and skin fibrosis in patients with diffuse systemic sclerosis. *Clin Exp Rheumatol* 2012; **30**: S17–S22.
11 Jonsdottir T, Gunnarsson I, Risselada A, Henriksson EW, Klareskog L, van Vollenhoven RF. Treatment of refractory SLE with rituximab plus cyclophosphamide: clinical effects, serological changes, and predictors of response. *Ann Rheum Dis* 2008; **67**: 330–334.
12 Tokunaga M, Saito K, Kawabata D *et al.* Efficacy of rituximab (anti-CD20) for refractory systemic lupus erythematosus involving the central nervous system. *Ann Rheum Dis* 2007; **66**: 470–475.
13 Merrill JT, Neuwelt CM, Wallace DJ *et al.* Efficacy and safety of rituximab in moderately-to-severely active systemic lupus erythematosus: the randomized, double-blind, phase II/III systemic lupus erythematosus evaluation of rituximab trial. *Arthritis Rheum* 2010; **62**: 222–233.
14 Tashkin DP, Elashoff R, Clements PJ *et al.* Effects of 1-year treatment with cyclophosphamide on outcomes at 2 years in scleroderma lung disease. *Am J Respir Crit Care Med* 2007; **176**: 1026–1034.
15 Volpe A, Ruzzenente O, Caramaschi P *et al.* Clinical associations of anti-CENP-B and anti-Scl70 antibody levels measured by multiplexed fluorescent microsphere immunoassay in systemic sclerosis. *Rheumatol Int* 2009; **29**: 1073–1079.

Akamata et al. Arthritis Research & Therapy 2014, 16:R86
http://arthritis-research.com/content/16/2/R86

arthritis research&therapy

RESEARCH ARTICLE Open Access

Bosentan reverses the pro-fibrotic phenotype of systemic sclerosis dermal fibroblasts via increasing DNA binding ability of transcription factor Fli1

Kaname Akamata, Yoshihide Asano*, Naohiko Aozasa, Shinji Noda, Takashi Taniguchi, Takehiro Takahashi, Yohei Ichimura, Tetsuo Toyama and Shinichi Sato

Abstract

Introduction: Although the pathogenesis of systemic sclerosis (SSc) still remains unknown, recent studies have demonstrated that endothelins are deeply involved in the developmental process of fibrosis and vasculopathy associated with SSc, and a dual endothelin receptor antagonist, bosentan, has a potential to serve as a disease modifying drug for this disorder. Importantly, endothelin-1 (ET-1) exerts a pro-fibrotic effect on normal dermal fibroblasts and bosentan reverses the pro-fibrotic phenotype of SSc dermal fibroblasts. The purpose of this study was to clarify the details of molecular mechanisms underlying the effects of ET-1 and bosentan on dermal fibroblasts, which have not been well studied.

Methods: The mRNA levels of target genes and the expression and phosphorylation levels of target proteins were determined by reverse transcription real-time PCR and immunoblotting, respectively. Promoter assays were performed using a sequential deletion of human α2 (I) collagen (COL1A2) promoter. DNA affinity precipitation and chromatin immunoprecipitation were employed to evaluate the DNA binding ability of Fli1. Fli1 protein levels in murine skin were evaluated by immunostaining.

Results: In normal fibroblasts, ET-1 activated c-Abl and protein kinase C (PKC)-δ and induced Fli1 phosphorylation at threonine 312, leading to the decreased DNA binding of Fli1, a potent repressor of the *COL1A2* gene, and the increase in type I collagen expression. On the other hand, bosentan reduced the expression of c-Abl and PKC-δ, the nuclear localization of PKC-δ, and Fli1 phosphorylation, resulting in the increased DNA binding of Fli1 and the suppression of type I collagen expression in SSc fibroblasts. In bleomycin-treated mice, bosentan prevented dermal fibrosis and increased Fli1 expression in lesional dermal fibroblasts.

Conclusions: ET-1 exerts a potent pro-fibrotic effect on normal fibroblasts by activating "c-Abl - PKC-δ - Fli1" pathway. Bosentan reverses the pro-fibrotic phenotype of SSc fibroblasts and prevents the development of dermal fibrosis in bleomycin-treated mice by blocking this signaling pathway. Although the efficacy of bosentan for dermal and pulmonary fibrosis is limited in SSc, the present observation definitely provides us with a useful clue to further explore the potential of the upcoming new dual endothelin receptor antagonists as disease modifying drugs for SSc.

* Correspondence: yasano-tky@umin.ac.jp
Department of Dermatology, University of Tokyo Graduate School of Medicine, 7-3-1 Hongo, Bunkyo-ku, Tokyo 113-8655, Japan

Introduction

Systemic sclerosis (SSc) is a multisystem connective tissue disease characterized by immune abnormalities, vascular injuries, and fibrosis of skin and certain internal organs [1]. Although the pathogenesis of SSc still remains unclear, it has been believed that fibroblast activation is a final consequence following inflammation, autoimmune attacks, and vascular damage. A wealth of evidence suggests that, once activated, SSc dermal fibroblasts establish a self-activation system by autocrine transforming growth factor (TGF)-β stimulation at least partially via upregulating cell surface receptors for latent-form TGF-β, such as integrin αVβ3, integrin αVβ5, and thrombospondin-1 [2-6]. A plausible strategy to treat fibrosis in SSc is to block the autocrine TGF-β signaling in SSc fibroblasts and better understanding of its molecular mechanism is necessary to develop the treatment for this complicated disorder [1,7].

The endothelins are a family of 21-amino-acid peptides mainly produced by endothelial cells, which consist of three isoforms, including endothelin-1 (ET-1) and the related peptides endothelin-2 and -3. In addition to a potent vasoconstrictive effect, ET-1 possesses a wide range of biological effects on different cell types. Several lines of evidence have demonstrated that ET-1 plays a pivotal role in the process of fibroblast activation as a downstream target of TGF-β [8-11]. TGF-β1 induces the expression of ET-1 through Smad- and activator protein-1/c-Jun N-terminal kinase-dependent signaling in human dermal fibroblasts, while through a Smad-independent ALK5/activator protein-1/c-Jun N-terminal kinase-dependent signaling in human lung fibroblasts, and the ability of TGF-β1 to trigger the pro-fibrotic gene program is dependent on ET-1 in both of these cells [9,12]. In animal models, forced expression of ET-1 accelerates dermal wound healing as well as TGF-β1, while blockade of endothelin signaling with bosentan, a dual endothelin receptor antagonist, significantly inhibits the effect of TGF-β1 on dermal wound healing [12]. Importantly, bosentan also attenuates bleomycin (BLM)-induced skin fibrosis in animal models [12]. Thus, endothelins are potentially implicated in the pathogenesis of fibrotic disorders.

The role of ET-1 has also been well-studied in SSc. Circulating ET-1 levels are elevated in diffuse cutaneous SSc and limited cutaneous SSc patients compared with healthy controls, and in limited cutaneous SSc patients with pulmonary arterial hypertension as compared to those without [13,14], suggesting the involvement of ET-1 in the development of fibrotic and vascular involvement associated with SSc. Clinically, bosentan has been shown to prevent the development of new digital ulcers in SSc patients by two high-quality randomized clinical trials [15,16]. As for pulmonary arterial hypertension associated with SSc, bosentan mostly prevents the exacerbation of hemodynamic parameters and improves exercise tolerance evaluated by 6-minute walk distance [17-19]. These clinical data suggest that bosentan is useful for the treatment of vascular involvement in SSc. In contrast, the clinical efficacy of bosentan for interstitial lung disease (ILD) is relatively limited [20,21], though bosentan reverses the pro-fibrotic phenotype of cultured SSc lung fibroblasts [8-11]. Since this discrepancy between experimental data and clinical observation may be partly due to the relatively lower tissue distribution of bosentan (approximately 1%) [22], endothelin receptor antagonists with better tissue distribution have a potential to improve the pathological fibrosis in SSc.

As described above, although ET-1 is a potent pro-fibrotic peptide and bosentan exerts a novel anti-fibrotic effect, the detailed molecular mechanism explaining these observations has still remained unknown. Therefore, we herein investigated the mechanisms by which ET-1 drives a pro-fibrotic gene program in normal dermal fibroblasts and bosentan reverses the pro-fibrotic phenotype of SSc dermal fibroblasts and the experimental dermal fibrosis in animal models.

Methods

Reagents

Anti-Fli1 antibody for immunoblotting and immunofluorescence and anti-protein kinase C (PKC)-δ antibody were purchased from Santa Cruz Biotechnology (Santa Cruz, CA, USA). Anti-Fli1 antibody for immunohistochemistry was obtained from BD Biosciences (San Diego, CA, USA). Antibodies against c-Abl and phospho-c-Abl (Tyr245) were bought from Cell Signaling (Danvers, MA, USA). Antibodies for β-actin and α-smooth muscle actin (α-SMA) and antibody for type I collagen were products from Sigma-Aldrich (St. Louis, MO) and Southern Biotech (Birmingham, AL, USA), respectively. The polyclonal rabbit anti-phospho-Fli1 (Thr312)-specific antibody was generated as described previously [23]. Bosentan was a gift from Actelion Pharmaceuticals (Allschwil, Switzerland). Smad3 inhibitor SIS3 was purchased from Calbiochem (San Diego, CA, USA).

Cell cultures

Human dermal fibroblasts were obtained by skin biopsy from the affected areas (dorsal forearm) of eight patients with diffuse cutaneous SSc with less than 2 years of skin thickening and from the corresponding area of eight closely matched healthy donors. Fibroblasts were cultured in Dulbecco's modified eagle medium with 10% fetal calf serum, 2 mM L-glutamine, and the antibiotic antimycotic solution. These cells were individually maintained as monolayers at 37°C in 95% air, 5% CO_2. All studies used cells from passage number three to six. The study was performed according to the Declaration of Helsinki and approved by the ethical committee of the University of Tokyo Graduate School of Medicine. Written informed consent was obtained from all of the patients and healthy controls.

Cell viability assay

Cell viability was evaluated by the trypan blue exclusion test. Cells were treated with the indicated concentration of bosentan. Cell viability was examined at 24 and 48 hours. Stained (dead) and unstained (viable) cells were counted with a hematocytometer.

Immunoblotting

Confluent quiescent fibroblasts were serum-starved for 48 hours and harvested. In some experiments, cells were stimulated with ET-1 or bosentan for the indicated period of time before being harvested. Whole cell lysates and nuclear extracts were prepared as described previously [2,24]. Samples were subjected to sodium dodecyl sulfate-polyacrylamide gels electrophoresis and immunoblotting with the indicated primary antibodies. Bands were detected using enhanced chemiluminescent techniques (Thermo Scientific, Rockford, IL, USA). According to a series of pilot experiments, anti-Fli1 antibody and anti-phospho-Fli1 (Thr312)-specific antibody work much better in immunoblotting using nuclear extracts and whole cell lysates, respectively.

RNA isolation and reverse transcription (RT) real-time PCR

Total RNA was isolated from normal and SSc fibroblasts with RNeasy spin columns (Qiagen, Crawley, UK). One μg of total RNA from each sample was reverse-transcribed into cDNA using the iScript cDNA synthesis kit (Bio-Rad, Hercules, CA, USA). Real-time quantitative PCR was performed using Fast SYBR Green PCR Master Mix (Applied Biosystems, Carlsbad, CA, USA) on ABI prism 7000 (Applied Biosystems) in triplicates. Human α2 (I) collagen (COL1A2) and Fli1 mRNA levels were normalized to human 18S rRNA mRNA levels. The sequences of primers for COL1A2, Fli1, and 18S rRNA were obtained from previous publications [25,26]. The ΔΔCt method was used to compare target gene and housekeeping gene (18S rRNA) mRNA expression.

Plasmid construction

Generation of a series of 5′-deletions of COL1A2/chloramphenicol acetyltransferase (CAT) construct consisting of the *COL1A2* gene fragments (+58 to −353, −264, −186, or −108 bp relative to the transcription start site) linked to the CAT reporter gene was done as previously described [27,28].

The evaluation of COL1A2 promoter activity by RT real-time PCR

Normal or SSc fibroblasts were grown to 50% confluence in 100-mm dishes, transfected with the indicated constructs along with pSV-β-galactosidase (β-GAL) using FuGENE6 (Roche Diagnostics, Indianapolis, IN, USA). After overnight incubation at 37°C, some cells were further stimulated with ET-1 or bosentan for 24 hours. The cells were harvested and CAT and β-GAL mRNA levels were determined using RT real-time PCR. Transfection efficiency was normalized by β-GAL mRNA levels. In some samples, it was confirmed that this method reproduces the results of relative promoter activity evaluated by the canonical method of CAT reporter assay using [^{14}C]-chloramphenicol. The sequences of primers were as follows: CAT forward 5′-TTCGTCTCAGCCA ATCCCTGGGTGA-3′ and reverse 5′-CCCATCGTGA AAACGGGGGCGAA-3′; β-GAL forward 5′-TCCACC TTCCCTGCGTTA-3′ and reverse 5′-AGAAGTCGGG AGGTTGCTG-3′.

DNA affinity precipitation assay

DNA affinity precipitation assay was performed as described previously [29]. Briefly, nuclear extracts prepared from dermal fibroblasts were incubated for 10 minutes at 4°C with gel shift binding buffer, and 20 μg of poly (dI-dC) in a final volume of 1 ml. Pre-clearing was performed by adding streptavidin-coupled agarose beads and incubating the mixture for 30 minutes at 4°C. After centrifugation, the supernatant was incubated with 500 pM of COL1A2-EBS oligonucleotide, which corresponds to bp −307 to −269 of COL1A2 promoter, or COL1A2-EBS-M oligonucleotide, which has a mutated Ets binding site (EBS) of COL1A2-EBS oligonucleotide, overnight at 4°C. Then, streptavidin-coated agarose beads were added, followed by a further 2-hour incubation at 4°C. The protein-DNA-streptavidin-agarose complex was washed twice with Tris-ethylenediaminetetraacetic acid (EDTA) including 100 mM NaCl, twice with gel shift binding buffer, and once with PBS. Precipitates were subjected to immunoblotting with anti-Fli1 antibody.

Chromatin immunoprecipitation (ChIP) assay

ChIP assay was carried out using EpiQuik ChIP kit (Epigentek, Farmingdale, NY, USA). Briefly, cells were treated with 1% formaldehyde for 10 minutes. The cross-linked chromatin was then prepared and sonicated to an average size of 300 to 500 bp. The DNA fragments were immunoprecipitated with anti-Fli1 antibody at 4°C. As a negative control, normal rabbit IgG was used. After reversal of crosslinking, the immunoprecipitated chromatin was quantified by RT real-time PCR. The primers were as follows: COL1A2/F-404, 5′-CTGGACAGCTCCTGCTTTGAT-3′; COL1A2/R-233, 5′-CTTTCAAGGGGAAACTCTGACTC-3′.

BLM-induced murine model of SSc

BLM (Nippon Kayaku, Tokyo, Japan) or PBS was injected subcutaneously into the back of C57BL/6 mice daily for 3 weeks, as described previously [30].

Immunohistochemistry

Immunohistochemistry with Vectastain ABC kit (Vector Laboratories, Burlingame, CA, USA) was performed on formalin-fixed, paraffin-embedded tissue sections using anti-Fli1 antibody according to the manufacturer's instruction.

Immunofluorescence

Rabbit anti-Fli1 antibody and mouse anti-α-SMA antibody were used as primary antibodies and Alexa Fluor 546 goat anti-rabbit IgG antibody (Invitrogen, Carlsbad, CA, USA) and fluorescein isothiocyanate (FITC)-conjugated rat anti-mouse IgG antibody (Roche) were used as secondary antibodies. Coverslips were mounted by using Vectashield with DAPI (Vector Laboratories), and staining was examined by using Bio Zero BZ-8000 (Keyence, Osaka, Japan) at 495 nm (green), 565 nm (red), and 400 nm (blue).

Statistical analysis

Statistical analysis was carried out with the Mann-Whitney *U*-test to compare the distributions of two unmatched groups. The paired *t*-test was used for the comparison of paired data after confirming the normal distribution. Statistical significance was defined as a *P*-value of <0.05.

Results

ET-1 rapidly induced the expression of type I collagen via the non-Smad signaling pathway

As an initial experiment, to determine the optimal dose of ET-1 to induce the expression of type I collagen in normal dermal fibroblasts, cells were treated with ET-1 at the concentration of 0, 50, 100, 200, or 400 nM for 24 hours and mRNA levels of the *COL1A2* gene were determined by RT real-time PCR. As shown in Figure 1A, ET-1 significantly increased the mRNA levels of the *COL1A2* gene at the concentration of 200 nM. To further confirm this finding at protein levels, the levels of type I collagen protein were determined by immunoblotting under the same conditions. As shown in Figure 1B, ET-1 induced the expression of type I collagen protein in a dose-dependent manner, reaching a peak at the concentration of 200 nM. Therefore, in the following studies, we stimulated cells with ET-1 at the concentration of 200 nM.

We next investigated the time course of ET-1-dependent induction of type I collagen in normal dermal fibroblasts. As shown in Figure 1C, the increase in the mRNA levels of the *COL1A2* gene was observed modestly but significantly as early as 15 minutes and reached a maximum around 30 to 60 minutes after the ET-1 stimulation. This observation was also reproduced at protein levels by immunoblotting (Figure 1D). As Smad3 has a big impact on the TGF-β-dependent regulation of type I collagen expression, we also investigated the effect of Smad3 inhibitor SIS3 on the ET-1-induced mRNA expression of the *COL1A2* gene. As shown in Figure 1E, SIS3 did not affect the mRNA levels of the *COL1A2* gene induced by ET-1 stimulation. Collectively, these results indicate that ET-1 rapidly increases the expression of type I collagen via the non-Smad signaling pathway.

The responsive element of COL1A2 promoter to ET-1 was located between −353 and −264 bp, which includes the Fli1 binding site

To identify potential regulatory elements of the *COL1A2* gene by ET-1, we performed a reporter analysis using a series of 5′-deletions of the COL1A2/CAT construct. As basal promoter activities of these constructs have been well-studied in our previous reports [31], we focused on the difference in the fold increase of each promoter activity induced by ET-1 stimulation. As shown in Figure 2, ET-1 significantly increased the promoter activity of the −353 COL1A2/CAT construct, whereas ET-1 totally lost its stimulatory effect on the promoter activity of the −264, −186, and −108 COL1A2/CAT constructs. These results indicate that the responsive element of COL1A2 promoter to ET-1 is located between −353 and −264 bp. Given that ET-1 increases the mRNA expression of the *COL1A2* gene independently of Smad3, ET-1 potentially exerts its stimulatory effect on the *COL1A2* gene by inactivating transcriptional repressor(s). As the binding site of Fli1, a potent repressor of the *COL1A2* gene, is located at −285 to −282 bp [32], we speculated that Fli1 may play a central role in the ET-1-dependent regulation of the *COL1A2* gene expression.

ET-1 induced the phosphorylation of Fli1 at threonine 312 and decreased its binding to the COL1A2 promoter

To confirm the hypothesis described above, we asked if ET-1 regulates the transcriptional activity of Fli1 in normal dermal fibroblasts. Our previous studies reported that transcriptional activity of Fli1 is tightly regulated by the phosphorylation-acetylation cascade triggered by PKC-δ-dependent phosphorylation of Fli1 at threonine 312 [23]. Phosphorylated Fli1 is subsequently acetylated by p300/CBP-associated factor at lysine 380, resulting in the loss of DNA binding ability [29] and degradation through the proteasomal pathway (unpublished data). As the phosphorylation of Fli1 at threonine 312 is a critical step regulating Fli1 transcriptional activity, we initially looked at the effect of ET-1 on the phosphorylation levels of Fli1 at threonine 312. As shown in Figure 3A, consistent with our hypothesis, Fli1 was phosphorylated at threonine 312 by ET-1 as early as 15 minutes after the stimulation. To further confirm if ET-1 decreases the binding ability of Fli1 to COL1A2 promoter, we employed the DNA affinity precipitation assay. As shown in Figure 3B, ET-1

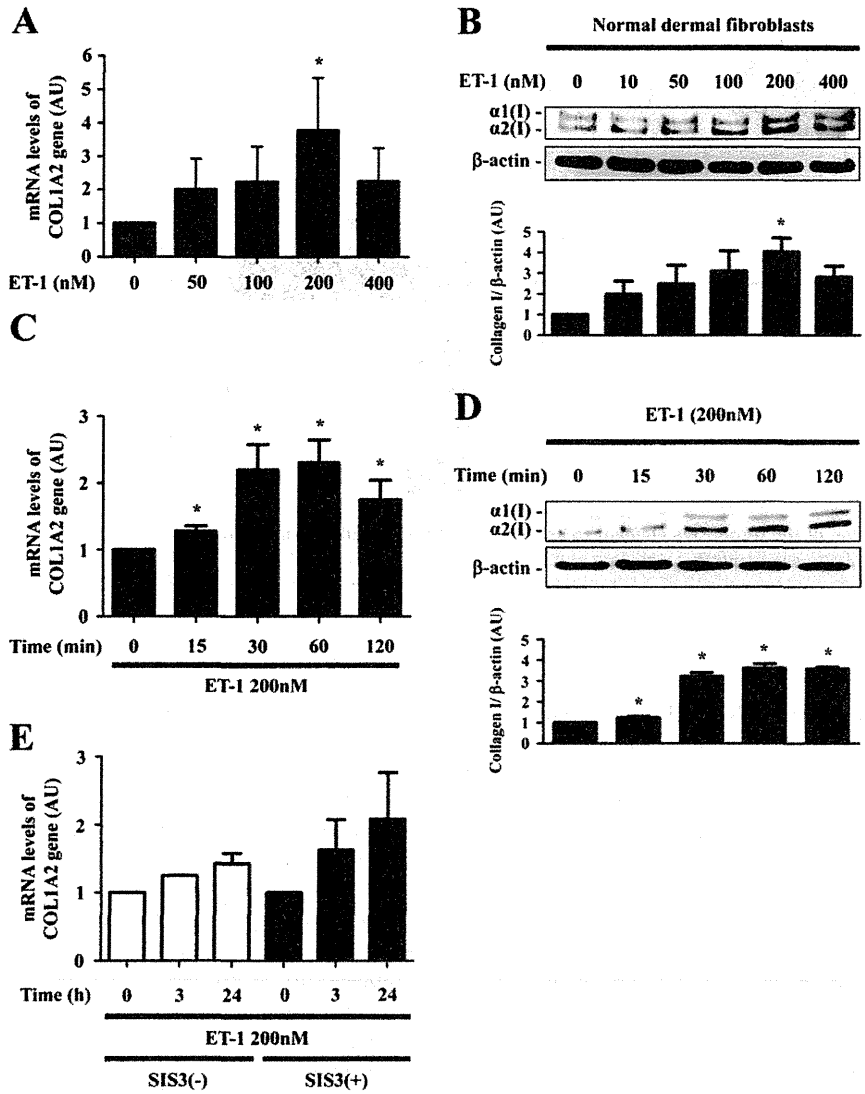

Figure 1 Endothelin-1 (ET-1) induced the expression of type I collage through the non-Smad pathway in normal dermal fibroblasts. **A, B.** Quiescent normal dermal fibroblasts were treated with the indicated concentration of ET-1 for 24 hours. mRNA levels of the human α2 (I) collagen (*COL1A2*) gene were determined by reverse transcription (RT) real-time PCR **(A)**. Under the same condition, whole cell lysates were subjected to immunoblotting with anti-type I collagen antibody **(B)**. **(C, D)** Quiescent normal dermal fibroblasts were treated with 200 nM of ET-1 for the indicated period of time. mRNA levels of the *COL1A2* gene **(C)** and the protein levels of type I collagen in whole cell lysates **(D)** were evaluated by RT real-time PCR and immunoblotting, respectively. **(E)** Quiescent normal dermal fibroblasts were treated with SIS3 (3 μM) or methanol. One hour later, some of the cells were treated with 200 nM of ET-1 for 3 or 24 hours. mRNA levels of the *COL1A2* gene were assessed by RT real-time PCR. The graph represents fold change in mRNA levels of the *COL1A2* gene and protein levels of type I collagen, which were quantified by densitometry, in response to ET-1 in comparison to unstimulated controls, which were arbitrarily set at 1. *P <0.05 versus control cells untreated with ET-1. α1(I), α1(I) procollagen; α2(I), α2(I) procollagen; AU, arbitrary unit.

stimulation decreased the DNA binding ability of Fli1 as early as 15 minutes, consistent with the results of immunoblotting. This observation was also confirmed *in vivo* by ChIP analysis showing that ET-1 decreased the association of Fli1 with the COL1A2 promoter at 3 hours after stimulation (Figure 3C). Taken together, these results indicate that ET-1 increases the promoter activity of the *COL1A2* gene by attenuating the DNA binding of Fli1 through its phosphorylation at threonine 312.

ET-1 promoted the nuclear localization of PKC-δ by activating c-Abl

We previously disclosed that sequential activation of c-Abl and PKC-δ is necessary for Fli1 phosphorylation at